5G fronthauls with multicore fibers: CPRI signals performance degradation induced by intercore crosstalk

João L. Rebola *[a,b], Tiago M. F. Alves[a,b], Adolfo V. T. Cartaxo[a,b], and André S. Marques[a]
[a]ISCTE-Instituto Universitário de Lisboa, Department of Information Science and Technology, Av. Forças Armadas, 1649-026, Lisbon, Portugal; [b]Instituto de Telecomunicações, Optical Communications Group, Av. Rovisco Pais, 1049-001, Lisbon, Portugal

ABSTRACT

Weakly-coupled multicore fibers (MCFs) have been proposed to support the huge data capacity demanded by future 5G fronthauls. However, in MCFs, intercore crosstalk (ICXT), i.e., power coupling between different MCF cores, can degrade significantly the performance of the 5G fronthaul, particularly, when using Common Public Radio Interface (CPRI) signals and direct-detection at the optical receiver. In this work, the performance degradation induced by ICXT in 5G fronthauls with MCFs and direct-detection is assessed by numerical simulation. We show that the study of the outage probability is essential to ensure the reliability and the good quality of service in 5G fronthauls supported by MCFs impaired by ICXT with CPRI signals transmission. The ICXT level that leads to an outage probability of 10^{-4} is more than 5.6 dB lower than the ICXT level necessary to reach the power penalty of 1 dB. Our results also indicate that fronthaul systems with lower extinction ratio exhibit an higher tolerance to ICXT.

Keywords: 5G wireless networks, Bit error rate, Common public radio interface, Intercore crosstalk, Multicore fiber, Outage probability, Power penalty.

1. INTRODUCTION

The emergence of 5G wireless networks and the continuous growth of traffic in communication networks[1,2] led to new proposals on the radio access networks architecture in order to increase data transmission efficiency and capacity. Cloud Radio Access Network (C-RAN) is expected to provide the 5G networks requirements in terms of network capacity, quality of service, latency and resources availability[2-5]. With the C-RAN architecture, a network segment known as fronthaul, which separates geographically, the base stations units (BBUs) hosted at the same location in a BBU pool, and the transmitter/receiver remote radio-head (RRH) antennas is deployed[2,4]. One way to cope with the high data transmission efficiency and capacity demanded for the fronthaul is to adopt solutions based on digital transmission over optical fiber such as, for example, the protocol defined at the Common Public Radio Interface (CPRI)[6]. The CPRI protocol is currently by far the most common standard for connecting BBUs to RRHs[2,5] and allows employing very small and cheap RRHs, since no digital processing functions are required at the RRHs[5]. The CPRI is a serial data rate protocol that defines the transmission of digitized samples of the radio signals using digital binary baseband signals, whose payload is known as I/Q data[6]. The CPRI signals transmission involves the use of intensity modulation at the optical transmitter and direct-detection at the receiver, being the on-off keying (OOK) modulation an attractive solution for its simpler and cheaper implementation. The 5G network fronthaul with CPRI protocol can demand very high capacities, depending on the radio-channel bandwidth, the number of sectors and number of antennas per sector[5]. For a radio-channel bandwidth of 1 GHz and with 256 antenna ports, the 5G fronthaul capacity must reach an aggregate capacity of 12.8 Tbps using the CPRI protocol[7]. This very high capacity is nowadays too hard to reach even considering the maximum CPRI signal bit rate of 24 Gbps per link[6] and transmission in single core fiber with conventional wavelength-division multiplexing (WDM), since the number of WDM channels required to reach such an aggregate capacity is above 500. Hence, several works have proposed to use multicore fibers (MCFs) in the fronthaul network segment to accomplish such high capacity[4,8,9].

Homogeneous weakly-coupled MCFs have been reported as a promising technology to expand transmission capacity. The cores of homogeneous MCFs have similar physical properties, which lead to similar propagation times for signals transmitted in different cores. In 5G fronthauls, this similarity can be explored to ensure low latency, and use specialized

*joao.rebola@iscte-iul.pt

transmission techniques and share receiver resources, as proposed for high capacity long-haul transmission[10,11]. In weakly-coupled MCFs, each single mode core guides one spatial mode, and the cores are sufficiently apart in the cladding, so that the power coupled from each core to other cores may be quite low[12,13]. Hence, the different cores can be used as independent channels. However, in weakly-coupled MCFs, the power coupling between cores, namely known as intercore crosstalk (ICXT), arises as a transmission impairment. ICXT is much stronger between adjacent cores than between non-adjacent cores, and its generation is distributed along the MCF[12,14]. Furthermore, the ICXT has a random time varying frequency dependence, which may cause the random appearance of high levels of ICXT in short periods of time[15-18]. Hence, the ICXT may affect severely the signal quality, particularly for MCFs with a large number of adjacent cores and for long link distances. As a consequence of the random evolution of ICXT along time, two ICXT effects should be considered when evaluating the MCF transmission system performance[19]. Over short periods of time, the Q-factor varies randomly[20] and this effect can be quantified by the degradation of the optical signal to noise ratio required for the same bit error rate (BER) in line-amplified transmission systems[19] or by the degradation of the receiver sensitivity in amplifier-less transmission systems. For an analysis over long periods of time, high levels of ICXT occurring in short time intervals appear and cause outage periods of system operation[16,19].

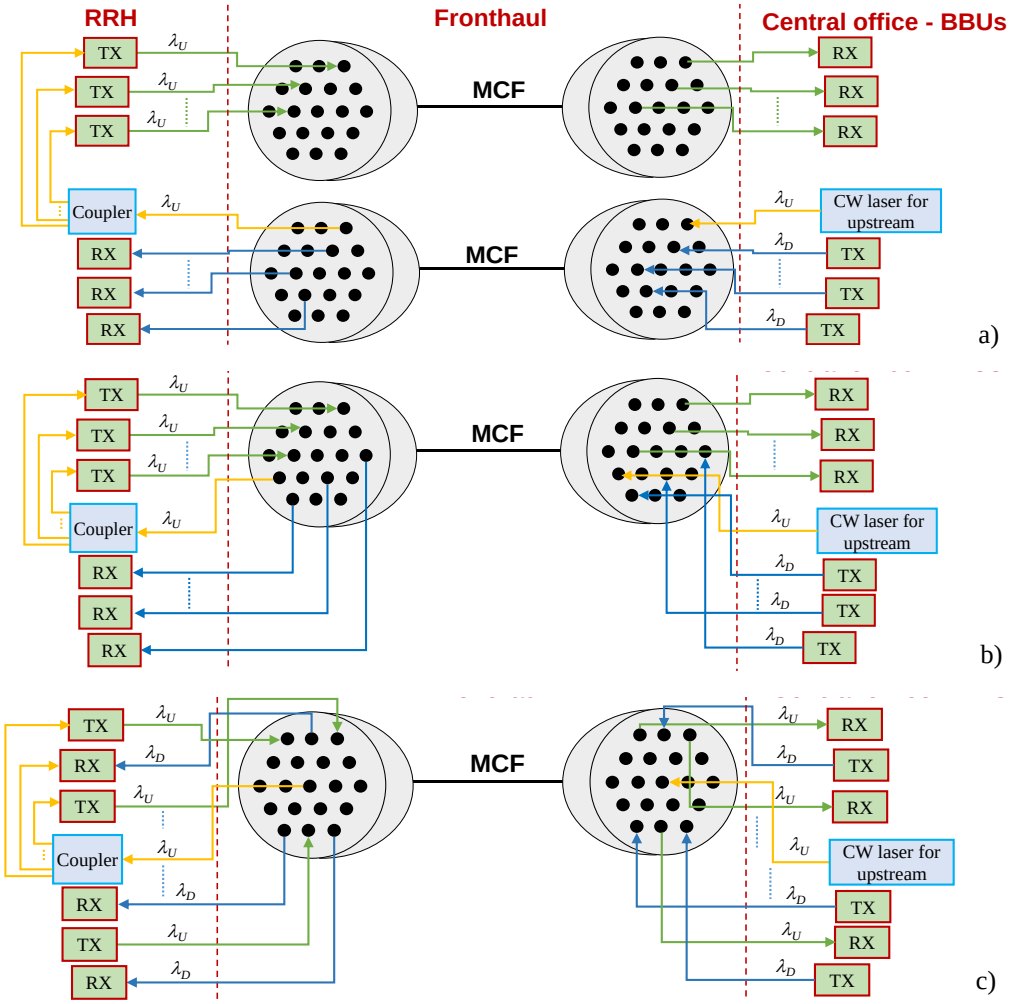

Figure 1. Different configurations for the 5G fronthaul with MCFs. a) Two MCFs are used in the fronthaul for duplex transmission. b) One MCF is used in the fronthaul for duplex-transmission: upper half cores are used for upstream transmission and lower half cores for downstream[4,9]. c) One MCF is used in the fronthaul for duplex-transmission: transmission directions are set in order that adjacent cores transmit in opposite directions in order to minimize ICXT[21]. In all three configurations, a single core is used to transmit a CW laser from the central office to the RRHs in order to provide the wavelength for the upstream direction. λ_U: upstream wavelength; λ_D: downstream wavelength; RX: receiver; TX: Transmitter.

Fig. 1 illustrates three possible configurations for the 5G fronthaul with MCFs. In all three configurations, it is assumed that a single wavelength is transmitted in a single core of the MCF. WDM solutions can be also envisioned, however, with higher cost. The wavelengths used for the downstream transmission, λ_D, are the same, which means that the transmitters for the downstream direction are equal. The same idea is considered for the upstream transmission in the upstream wavelength λ_U. This wavelength is provided by the central office from a continuous-wave (CW) laser source through transmission in a single dedicated MCF core and is distributed to the upstream transmitters. For connecting the MCFs to external equipment, MCF connectors are assumed (which are not depicted in Fig. 1). Fig. 1 a) shows the configuration where, to guarantee duplex-transmission, one MCF is used for each transmission direction. Fig. 1 b) depicts the 5G fronthaul configuration that utilizes only one MCF to ensure duplex transmission: the upper cores are used for upstream transmission and the lower cores are used for downstream transmission[4,9]. Fig. 1 c) illustrates a 5G fronthaul ICXT-"aware" configuration using one MCF, as it explores the fact that transmitting signals in opposite directions in adjacent cores reduces the ICXT effect[21]. Hence, in this configuration, the transmission directions in adjacent cores are set interchangeably in opposite directions. Even though, with this configuration, when many cores are used for transmission, the same transmission direction is employed in some adjacent cores.

In this work, we numerically investigate the transmission of 10 Gbps CPRI signals along 5G fronthauls supported by weakly-coupled MCFs systems with direct-detection and how the ICXT affects the transmitted signal performance. Numerical results are obtained through the combination of Monte Carlo (MC) simulation to assess the ICXT impact on the performance, with a semi-analytical method for noise evaluation. The performance metrics used for this assessment are the BER, power penalty and outage probability. This paper is organized as follows. Section 2 presents the fronthaul equivalent simulation model and the procedure for the BER estimation. Section 3 presents and discusses the numerical results. Section 4 provides the conclusions.

2. SYSTEM MODEL AND BER CALCULATION

In this section, the communication system model developed to assess the impact of ICXT on the performance of a 5G fronthaul with direct-detection supported by weakly-MCFs is described. The BER estimation using simulation of the signal and ICXT combined with a semi-analytical method to account for the electrical noise influence is also explained.

2.1 System model

For assessing the impact of ICXT on the 5G fronthaul performance, where an OOK signal following the CPRI protocol is transmitted, we consider only a single interfering signal transmitted in the interfering core *m* that may degrade the performance of other similar CPRI signal transmitted in the interfered core *n*. An extension of the main results to multiple interfering cores is presented in subsection 3.2.

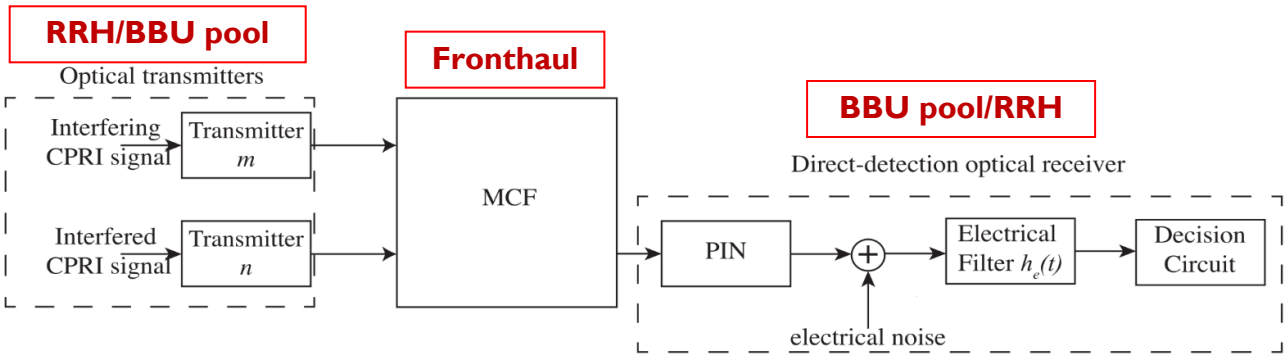

Figure 2. Equivalent system model with two interfering cores used to study the impact of ICXT on a 5G fronthaul with weakly-coupled MCF and direct detection.

Fig. 2 depicts the equivalent system model used to study the impact of ICXT on the OOK signal transmission performance in 5G fronthauls with MCFs and direct-detection. As each CPRI link is assigned to a single core of the

MCF to perform a connection between the pool of BBUs and one RRH, our model considers a point-to-point link between the transmitter and the receiver to transmit the OOK signal. This model can be applied for both downstream (BBU pool to RRH) or upstream (RRH to BBU pool) directions. As shown in Fig. 2, two ideal chirpless optical transmitters, which perform linear conversion from the electrical domain to the optical domain, generate an OOK signal with rectangular pulse shape and arbitrary extinction ratio for its respective cores, the interfered core *n* and the interfering core *m*. The OOK signals at the input of cores *n* and *m* are generated with the same CPRI bit rate and their bit transitions are assumed aligned in time.

To model the MCF, in core *n*, only propagation delay and fiber dispersive (up to second order) effects are considered. The same fiber attenuation is assumed for the two cores. Hence, the fiber attenuation level is not relevant in our analysis, as the average signal power at the optical receiver input, i.e., the receiver sensitivity is considered to obtain the system performance. We model the ICXT by the discrete changes model developed for signals with dual-polarization[22]. To keep the complexity and time of simulation at acceptable levels, we analyse the evolution of the impact of ICXT on system performance in time fractions (corresponding to the duration of several thousand of bits, i.e., much shorter than the ICXT decorrelation time), separated by time intervals longer than the decorrelation time of ICXT of the MCF. This means that, from time fraction to time fraction, the ICXT is uncorrelated and, within each time fraction, is totally correlated. This simplifies the simulation of the ICXT as, in each time fraction, from the ICXT viewpoint, one MCF realization is generated that is uncorrelated to all other MCF realizations associated with other fractions of time. In this case, in each time fraction, a MCF realization, corresponding to the interfering signal in core *n* resulting from ICXT caused by the signal in core *m*, is obtained from the ICXT field transfer functions referring to the polarization directions **x** and **y** from[22]

$$F_{a,b}(\omega) = -j\frac{K_{nm}}{\sqrt{2}}e^{-j\beta_n(\omega)L}\sum_{k=1}^{N_p}e^{-jd_{mn}\omega\cdot z_k}e^{-j\phi_k^{(a,b)}} \quad (1)$$

where $a,b \in \{x,y\}$, $\beta_n(\omega)$ is the average intrinsic propagation constant of the two polarizations of core *n*, K_{nm} is the average discrete coupling coefficient of the two polarizations, z_k is the longitudinal coordinate of the *k*-th point between consecutive phase-matching points (PMPs), N_p is the number of PMPs, L is the MCF length and $\phi_k^{(a,b)}$ is the *k*-th random phase shift (RPS), associated with the *k*-th PMP[22]. Each RPS is modelled by a random variable uniformly distributed between $[0,2\pi[$ and different RPS are uncorrelated[22]. The skew between cores *m* and *n* is defined by $S_{mn} = d_{mn}\cdot L$, with d_{mn} the average walkoff parameter between cores *m* and *n*. For equal powers at the MCF cores input and same core losses, the ratio between the average crosstalk power at the output of the interfered core *n* and the average power of the signal at the output of the interfering core *m*, X_c, is related to the parameters of Eq. (1) by $X_c = N_p|K_{nm}|^2$.[12,14] In this study, we consider that the crosstalk level induced by fan-in and fan-out devices needed for MCF coupling, where the crosstalk is originated in a localized manner[15], is much lower than the ICXT level induced by MCF, where the ICXT is generated in a distributed way along the fiber length[15]. Hence, the effect of fan crosstalk may be neglected in the scope of our analysis. To obtain the interfering signal at the output of core *n* resulting from ICXT caused by the signal in core *m*, we pass the signal at the input of core *m* by the filter with transfer function given by Eq. (1). The different MCF realizations are obtained by generating randomly different sets of N_p RPSs. In each iteration of the MC simulator, one MCF realization is generated, and the bits of the interfering CPRI signal transmitted in core *m* are randomly generated.

At the optical receiver input, the signal impaired by ICXT is photodetected by a PIN with unit responsivity and bandwidth much larger than the CPRI signal bit rate to avoid intersymbol interference (ISI) from lowpass filtering. The signal at the PIN output is filtered by an electrical filter modelled by a 4th order Bessel filter with a −3 dB cut-off frequency equal to the OOK signal bit rate, R_b. The electrical noise, referred to the electrical filter input, is characterized by a noise equivalent power of 1×10^{-12} W/Hz$^{1/2}$.[23] After electrical filtering, at the decision circuit, the received signal is sampled at the time instants $t_l = t_{opt} + lT_b$, where t_{opt} is the optimum sampling time extracted from the eye-pattern obtained in the simulation (different from MCF realization to MCF realization), T_b is the bit period and $l = 1, 2, \ldots, N_b$, with N_b, the number of bits considered for BER assessment in each MCF realization.

2.2 Semi-analytical BER estimation

To assess the BER, we use MC simulation combined with a semi-analytical technique[23]. The impact of electrical noise from the receiver on the BER is taken into account analytically, and fiber chromatic dispersion and ICXT effects on the BER are evaluated using waveform simulation in each MC simulation iteration. Let i denote the i-th iteration of the MC simulator, in which a different MCF realization is generated using Eq. (1). The BER of the i-th iteration is given by[23]

$$BER_i = \frac{1}{N_b}\left\{\sum_{\substack{l=1\\ j=0}}^{N_b} Q\left(\frac{F_i - m_{0,l,i}}{\sigma_{0,l,i}}\right) + \sum_{\substack{l=1\\ j=1}}^{N_b} Q\left(\frac{m_{1,l,i} - F_i}{\sigma_{1,l,i}}\right)\right\} \tag{2}$$

where $Q(x)$ is the Q-function[23], $m_{j,l,i}$ and $\sigma_{j,l,i}$ are the mean and standard deviation of the current at the decision circuit input at the time instants t_l, conditioned on the transmitted bit j (0 or 1). As we consider electrical noise only, $\sigma_{0,l,i} = \sigma_{1,l,i}$. The ICXT and ISI from fiber dispersion affect the mean $m_{j,l,i}$ components as waveform distortion, which is taken from the eye-pattern obtained in the simulation at time instants t_l. The decision threshold F_i is optimized in each iteration of the MC simulator using the bisection method to minimize the BER per MCF realization. The average BER is defined by

$$\overline{BER} = \frac{1}{N_{MCF}} \cdot \sum_{i=1}^{N_{MCF}} BER_i \tag{3}$$

with the parameter N_{MCF} defining the MC simulator number of iterations.

3. NUMERICAL RESULTS AND DISCUSSION

In this section, the impact of ICXT on the performance of CPRI signals transmitted in 5G fronthauls supported by weakly-coupled MCFs is investigated by numerical simulation by obtaining the power penalty and the outage probability due to ICXT. The simulation parameters that are kept constant throughout this work are shown in Table 1.The CPRI bit rate option 8,[6] with R_b = 10.1376 Gbps, 64B/66B line coding and forward-error correction (FEC) is chosen for this work. CPRI bit rates near 10 Gbps per MCF core have been chosen, since this bit rate has been already studied for the fronthaul of 5G networks with single core fibers[3,24]. Furthermore, this bit rate is the most common found in optical fiber telecommunication systems with OOK signal transmission and direct-detection, hence, leading to a simpler and cheaper implementation. We assume a target average pre-FEC BER of 10^{-3}.[19] An identical fiber dispersion parameter is considered for the two cores. The length of the MCF is set for the maximum reach defined for the 5G fronthaul[7] and originates a slight ISI due to chromatic dispersion at the CPRI bit rate investigated. The number of PMPs is set to characterize accurately the mechanism of the RPSs[14]. The number of generated OOK bits per MCF realization is set to take into account the ISI of the communication system in a rigorous way[23]. Two different skews are considered: a skew shorter than the bit period, $S_{mn} \cdot R_b \approx 0.2$, which corresponds to d_{mn} = 1 ps/km; and a skew much higher than the bit period, $S_{mn} \cdot R_b \approx 10$ obtained with d_{mn} = 50 ps/km. With this, we are analysing two situations: (i) bit rate of the CPRI signal much higher than the ICXT decorrelation bandwidth and (ii) bit rate of the CPRI signal much lower than the ICXT decorrelation bandwidth. The number of MC simulation iterations needed to obtain a stabilized value of the average BER is set to 10^3 as a conservative choice for the CPRI signal with 10.1376 Gbps[23].

Table 1. Simulation parameters.

Parameter	Value
Option 8 CPRI bit rate	10.1376 Gbit/s
Carrier wavelength	1550 nm
Fiber dispersion parameter	17 ps/nm/km
Fiber attenuation coefficient	0.2 dB/km
Fiber length	20 km
Number of PMPs	1000
Number of generated OOK bits per MCF realization	2^9
Number of MCFs iterations per average BER	10^3

3.1 Power penalty due to ICXT

In this subsection, the power penalty due to ICXT is studied. The power penalty due to ICXT is defined as the ratio between the average powers at the optical receiver input needed to reach a target average BER of 10^{-3} with and without ICXT, respectively[23]. Fig. 3 depicts the power penalty due to ICXT as a function of the crosstalk level, for $S_{mn}{\cdot}R_b \approx 0.203$ and $S_{mn}{\cdot}R_b \approx 10.139$. Figs. 3 a) and b) correspond to the power penalty obtained with $r = \infty$ and $r = 10$, respectively. The receiver sensitivity to reach the target average BER is −31.14 dBm, for $r = \infty$, and −30.46 dBm, for $r = 10$. The 1 dB power penalty is defined as a reference for determining the maximum tolerable ICXT level[23]. Fig. 3 shows that the power penalty only becomes significant for very high ICXT levels above −14 dB. In Fig. 3 a), for $r = \infty$, the maximum tolerable ICXT level is around −14 dB, for $S_{mn}{\cdot}R_b \approx 0.203$, and around −13.5 dB, for $S_{mn}{\cdot}R_b \approx 10.138$. For $S_{mn}{\cdot}R_b \approx 10.139$, the ICXT effect on the power penalty is lower than with $S_{mn}{\cdot}R_b \approx 0.203$. Fig. 3 b) shows that the effect of ICXT is lessened with the extinction ratio reduction and it leads to similar power penalties for the two $S_{mn}{\cdot}R_b$. The maximum tolerable ICXT level is around −12 dB.

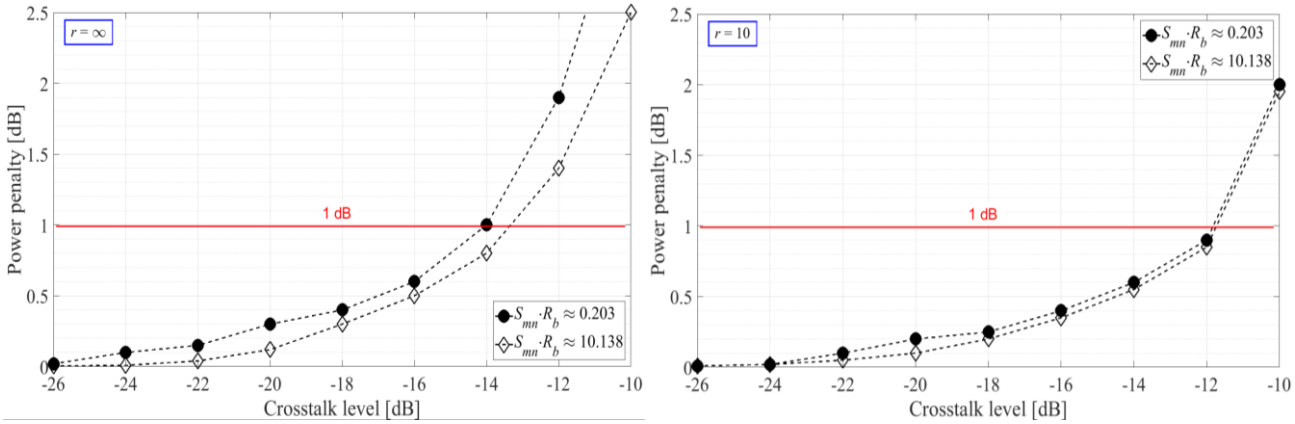

Figure 3. Power penalty as a function of crosstalk level, X_c, for a target average BER of 10^{-3}, corresponding to a) $r = \infty$ and b) $r = 10$, for $S_{mn}{\cdot}R_b \approx 0.203$ (circles) and $S_{mn}{\cdot}R_b \approx 10.138$ (diamonds).

3.2 Outage probability

Several works[15,18] have shown that ICXT can degrade severely the BER during random fractions of time, leading to system unavailability during these time fractions. Hence, it is important to study the system unavailability when dealing with ICXT. A typical metric for measuring the unavailability of a communication system over a certain time interval is the outage probability[19,25]. The outage probability is the probability of the system being unavailable for a target BER limit. In the simulation, the outage probability is estimated by counting the number of MCF realization occurrences that lead to a BER above the BER limit and dividing this number by the total number of MCF realizations. In our simulations, we have seen that 200 occurrences are enough to obtain reasonably accurate estimates of the outage probability[23]. The following results consider a BER in the absence of ICXT of 10^{-5}, and the system is considered to be unavailable when a MCF realization leads to a BER that overcomes the BER limit of 10^{-3}.

Fig. 4 shows the outage probability as a function of the crosstalk level, for a) $r = \infty$ and b) $r = 10$, with $S_{mn}{\cdot}R_b \approx 0.203$ and $S_{mn}{\cdot}R_b \approx 10.138$. In absence of ICXT, the signal power at the optical receiver input is set to −29.42 dBm and −28.90 dBm, respectively, for a) $r = \infty$ and b) $r = 10$, to reach a BER of 10^{-5}. To reach outage probabilities below 10^{-5}, due to the unfeasible required computational time, a cubic interpolation of the $\log_{10}(\,)$ of the outage probability obtained by MC simulation is used. Then, outage probabilities below 10^{-5} are obtained by extrapolation. Fig. 4 shows that, for high ICXT levels ($X_c > -12$ dB), the system becomes unavailable with a very high probability near 10^{-1}. For lower ICXT levels, with $S_{mn}{\cdot}R_b \approx 0.203$, the system is less tolerant to ICXT than with $S_{mn}{\cdot}R_b \approx 10.138$, for both extinction ratios. For example, for the typical outage probability considered in optical communications systems[25], of 10^{-4}, and $r = \infty$, the maximum tolerable crosstalk level is −23.2 dB, for $S_{mn}{\cdot}R_b \approx 0.203$, and −19.2 dB, for $S_{mn}{\cdot}R_b \approx 10.138$. This corresponds to a difference between the maximum tolerable ICXT levels obtained for the two skews of about 4 dB. Fig. 4 b) shows that, for $r = 10$, the tolerance to ICXT is improved in comparison with $r = \infty$. For the outage probability of 10^{-4}, the

maximum tolerable crosstalk level is −21.3 dB, for $S_{mn}{\cdot}R_b \approx 0.203$, and −17.9 dB, for $S_{mn}{\cdot}R_b \approx 10.138$, which in comparison with $r = \infty$, gives an improved tolerance of 1.9 dB and 1.3 dB, respectively, for $S_{mn}{\cdot}R_b \approx 0.203$ and $S_{mn}{\cdot}R_b \approx 10.138$. The difference between the tolerated ICXT level obtained with the two skews, for $r = 10$, has diminished to about 3.4 dB, when compared to the one obtained for $r = \infty$. It should be emphasized that the results obtained for the outage probability have been compared with experimental results[26] and discrepancies regarding the ICXT level that leads to a specific outage probability below 1 dB have been found.

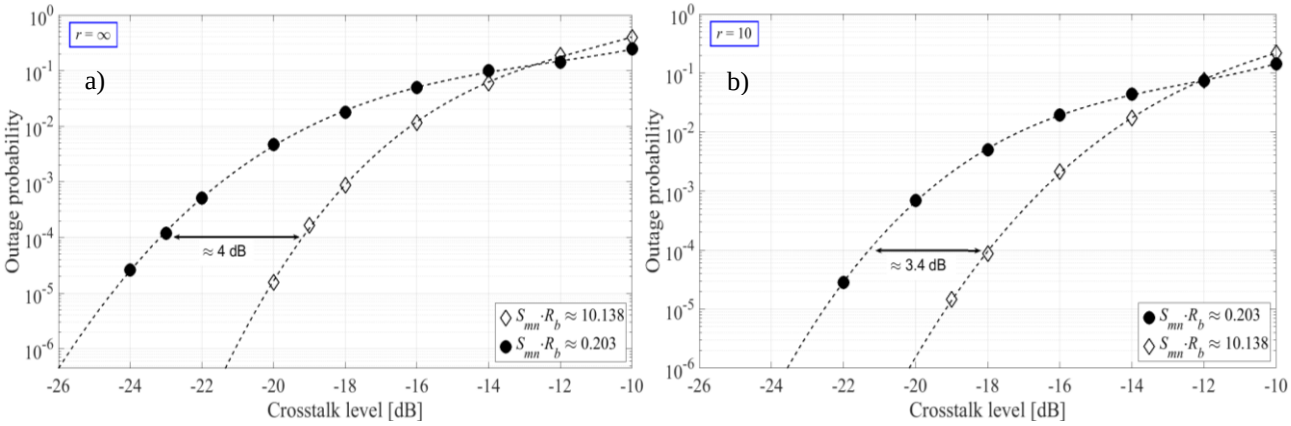

Figure 4. Outage probability as a function of the crosstalk level, X_c, for a BER in the absence of ICXT of 10^{-5} and a BER limit of 10^{-3}, corresponding to a) $r = \infty$ and b) $r = 10$, for $S_{mn}{\cdot}R_b \approx 0.203$ (circles) and $S_{mn}{\cdot}R_b \approx 10.138$ (diamonds). The dashed lines represent a cubic interpolation of the $\log_{10}(\ )$ of the outage probability.

From Fig 4, to ensure an outage probability of 10^{-4}, the ICXT level must be below −23.2 dB, for the two skews and extinction ratios, for one single interfering core. For this ICXT level, the power penalty due to ICXT is negligible, as shown in Fig. 3. A power penalty of 1 dB is only reached when the crosstalk level is above −14 dB. For this high ICXT level, Fig. 4 shows a very high outage probability, being its minimum near $1{\times}10^{-2}$ in Fig. 4 b).

The conclusion regarding the maximum ICXT level achievable for a pre-defined outage probability can be extrapolated to a MCF with N_i interfering cores. Consider that the interfering signals have the same power, the ICXT induced by each different interfering core is independent from the one induced by other cores, and the ICXT levels induced by each interfering core are equal. Under these conditions, a worst-case approach for the maximum tolerable ICXT level induced by each interfering core is given by $X_{c,max}$ [dB] $\leq X_{c,max,1}$ [dB] + $10{\cdot}\log10(N_i)$, where $X_{c,max,1}$ denotes the maximum tolerable ICXT level obtained for a single interfering core. For $X_{c,max,1} = -23.2$ dB, for the outage probability of 10^{-4}, a MCF with 4 interfering cores in one interfered test core, will have a worst-case predicted maximum tolerable ICXT level per each interfering core of −29.2 dB.

4. CONCLUSIONS

In this work, the transmission of 10 Gbit/s OOK signals adopting the CPRI protocol in a 5G fronthaul supported by weakly-coupled MCFs has been investigated. We have shown that, in such systems, due to the random nature of ICXT, the study of the outage probability is essential to ensure a good performance. During significant fractions of time, the system can be unavailable due to ICXT, even if the average BER designed for the system is accomplished. To get an acceptable outage probability of 10^{-4}, the ICXT level must be maintained below −21.3 dB, for r =10, and −23.2 dB, for $r = \infty$, for fronthauls with low $S_{mn}{\cdot}R_b$. For fronthauls with higher $S_{mn}{\cdot}R_b$, as the ICXT effect is reduced, the maximum tolerated ICXT level is increased to −17.9 dB, for r =10, and −19.2 dB, for $r = \infty$. For all the ICXT levels limits obtained using the reference outage probability of 10^{-4}, the estimated power penalty due to ICXT is almost negligible, below 0.5 dB. To reach noticeable values of power penalty, for a target BER of 10^{-3}, the ICXT level must be increased at least to −14 dB to reach the 1 dB power penalty. For such high ICXT level, the outage probability is above $1{\times}10^{-2}$ in all scenarios studied, which is unacceptable. Hence, this work shows that the two performance metrics predict maximum tolerable ICXT levels very discrepant with minimum differences above 5.6 dB, when comparing the same 5G fronthaul system, i.e., with the same extinction ratio and skew. So, as a main conclusion of this work, due to the random behavior

of ICXT, the planning of OOK signaling direct-detection optical communication systems supported by weakly-coupled MCFs, should take into account the outage probability due to ICXT. Even if the system is designed for an acceptable power penalty of 1 dB, for the ICXT levels that lead to this penalty, the outage probability can be very high and unacceptable. Other noteworthy conclusion taken from the results presented in this work is that systems with lower extinction ratio exhibit higher tolerance to ICXT.

ACKNOWLEDGEMENTS

This work was supported in part by Fundação para a Ciência e a Tecnologia (FCT) from Portugal under the project of Instituto de Telecomunicações AMEN-ID/EEA/50008/2013.

REFERENCES

[1] China Mobile," C-RAN: the road towards green RAN," White Paper, version 2.5, https://pdfs.semanticscholar.org/eaa3 (2011).
[2] Pizzinat, A., Chanclou, P., Saliou F. and Diallo, T., "Things you should know about fronthaul," IEEE/OSA J. Lightw. Technol., 33(5), 1077–1083 (2015).
[3] Chanclou, P., Pizzinat, A., Clech, F., Reedeker, T., Lagadec, Y., Salliou F., Guyader, B., Guillo, L., Deniel, Q., Gosselin, S., Le, S., Diallo, T., Brenot, R., Lelarge, F., Marazzi, L., Parolari, O., Martinelli, M., Dull, S., Gebrewold, S., Hillerkuss, D., Leuthold, J., Gavioli, G. and Galli, P., "Optical fiber solution for mobile fronthaul to achieve cloud radio access network," Future Network and Mobile Summit 2013, session 9e (2013).
[4] Galve, J.M., Gasulla, I., Sales, S. and Capmany, J., "Reconfigurable radio access networks using multicore fibers," IEEE J. Quantum Electron., 52(1), 1–7 (2016).
[5] Alimi, I., Teixeira, A. and Monteiro, P., "Towards an efficient C-RAN optical fronthaul for the future networks: a tutorial on technologies, requirements, challenges and solutions," IEEE Commun. Surveys Tuts., 20(1), 708–769 (2018).
[6] Common Public Radio Interface: CPRI Specification V7.0. Standard Document Specification, vol. 1, (2015).
[7] Telecommunications Standardization Sector of ITU-T, "Transport network support of IMT-2020/5G," ITU-T Technical Report, https://www.itu.int/md/T17-SG15-170619-TD-GEN-0078/en (2018).
[8] Macho, A., Morant, M. and Llorente, R., "Next-generation optical fronthaul systems using multicore fiber media," IEEE/OSA J. Lightw. Technol., 34(20), 4819–4827 (2016).
[9] Galve, J., Gasulla, I., Sales., S. and Capmany, J., "Fronthaul design for radio access networks using multicore fibers," Waves Magaz., 7(1), 69–80 (2015).
[10] Puttnam, B., Luís, R., Mendinueta, J., Sakaguchi, J., Klaus, W., Awaji, Y., Wada, N., Kanno, A. and Kawanishi, T., "High-capacity self-homodyne PDM-WDM-SDM transmission in a 19-core fiber," Opt. Expr., 22(18), 21185–21191 (2014).
[11] Feuer, M., Nelson, L., Zhou, X., Woodward, S., Isaac, R., Zhu, B., Taunay, T., Fishteyn, M., Fini, J. and Yan, M., "Joint digital signal processing receivers for spatial superchannels," IEEE Photon. Techn. Lett., 24(21), 1957–1960 (2012).
[12] Hayashi, T., Taru, T., Shimakawa, O., Sasaki, T. and Sasaoka, E., "Design and fabrication of ultra-low crosstalk and low-loss multicore fiber," Opt. Expr., 19(17), 16576-16592 (2011).
[13] Tu, J., Saitoh, K., Koshiba, M., Takenaga, K. and Matsuo, S., "Design and analysis of large-effective-area heterogeneous trench-assisted multi-core fiber," Opt. Expr., 20(14), 15157-15170 (2012).
[14] Cartaxo, A., Luís, R., Puttnam, B., Hayashi, T., Awaji, Y. and Wada, N., "Dispersion impact on the crosstalk amplitude response of homogeneous multi-core fibers," IEEE Photon. Technol. Lett., 28(17), 1858–1861 (2016).
[15] Luís, R., Puttnam, B., Cartaxo, A., Klaus, W., Mendinueta, J., Awaji, Y., Wada, N., Nakanishi, T., Hayashi, T. and Sasaki, T., "Time and modulation frequency dependence of crosstalk in homogeneous multi-core fibers," IEEE/OSA J. Lightw. Technol., 15(2), 441–447 (2016).
[16] Alves, T., Cartaxo, A., Luís, R., Puttnam, B., Awaji, Y. and Wada, N., "Intercore crosstalk in direct-detection homogeneous multicore fiber systems impaired by laser phase noise," Opt. Expr., 25(23), 29417-29431 (2017).
[17] Alves, T. and Cartaxo, A., "Intercore crosstalk in homogeneous multicore fibers: theoretical characterization of

stochastic time evolution,". IEEE/OSA J. Lightw. Technol., 35**(**21), 4613-4623 (2017).
[18] Alves, T. and Cartaxo, A., "Characterization of the stochastic time evolution of short-term average intercore crosstalk in multicore fibers with multiple interfering cores," Opt. Expr., 26(4), 4605-4620 (2018).
[19] Puttnam, B., Luís, R., Eriksson, T., Klaus, W., Mendinueta, J., Awaji, Y. and Wada, N., "Impact of inter-core crosstalk on the transmission distance of QAM formats in multi-core fibers," IEEE Photon. J., 8(5), Art. ID. 0601109 (2016).
[20] Hayashi, T., Sasaki, T. and Sasaoka, E., "Behavior of inter-core crosstalk as a noise and its effect on Q-factor in multi-core fiber," IEICE Trans. Commun., E97-B(5), 936–944 (2014).
[21] Sano, A., Takara, H., Kobayashi, T. and Miyamoto, Y., "Crosstalk-managed high capacity long haul multicore fibre transmission with propagation-direction interleaving," IEEE/OSA J. Lightw. Technol., 32(16), 2771–2779 (2014).
[22] Soeiro, R., Alves, T. and Cartaxo, A., "Dual polarization discrete changes model of inter-core crosstalk in multi-core fibers," IEEE Photon. Technol. Lett., 29**(**16), 1395-1398 (2017).
[23] Marques, A., Rebola, J. and Cartaxo, A., "Transmission of CPRI signals along weakly-coupled multicore fibers for support of 5G networks," Proc. International Conference on Transparent Optical Networks, ICTON 2018, paper We.B2.7 (2018).
[24] Parolari, P., Marazzi, L., Brunero, M., Martinelli, M., Maho, A., Barbet, S., Lelarge, F., Brenot, R., Gavioli, G., Simon, G., Saliou, F., Deniel, Q. and Chanclou, P., "Operation of RSOA WDM PON self-seeded transmitter over more 50 km of SSMF up to 10 Gb/s," Proc. Optical Networking and Communication Conference and Exhibition, OFC 2014, paper W3G.4 (2014).
[25] Winzer, P. and Foschini, G., "MIMO capacities and outage probabilities in spatially multiplexed optical transport systems," Opt. Expr., 19(17), 16680–16696 (2011).
[26] Alves, T., Rebola, J. and Cartaxo, A., "Outage probability due to intercore crosstalk in weakly-coupled MCF systems with OOK signalling," accepted for publication in Optical Networking and Communication Conference and Exhibition, OFC 2019.